43rd AIAA Aerospace Sciences Meeting and Exhibit, 10 - 13 Jan 2005, Reno, Nevada AIAA2005-0679

An Electrostatically Activated Resonant Micropump-mixer

Chia-Wen Tsao* and Kamran Mohseni†

Department of Aerospace Engineering,University of Colorado, Boulder, CO 80309-429.

An active mixing and pumping strategy is proposed to enhance mixing of two fluids through vortex formation and accumulation. A resonant micropump-mixer is designed and fabricated, where an electrostatically activated plate is placed at or in close vicinity of the interface between the two incoming streams at the junction of a Y- or T-shaped microchannel. Mixing is enhanced by increased interface area between the two fluids during the vortex formation at the tip of the resonant plate. Several packaging techniques are employed so that the two initially segregated streams flow underneath and above the resonant plate. Fabrication of the micropump-mixer is achieved in two steps. Commercial PolyMUMPs process is initially used to fabricate a resonant plate. The resonant plate is then flip-chip bonded into a prefabricated microchannel. The Laser Induced Fluorescence (LIF) technique is used for flow visualization and characterization, where effective mixing and pumping capabilities of the micropump-mixer are demonstrated.

Nomenclature

$\bar{x}$	nondimensional distance x/L
C	Concentration gradient
D	Diffusion coefficient
d	Tip deflection
E	Moment of inertia
f	Frequency
g	Gap between the plate and the electrode
h	Thickness of the resonant plate
I	Module of elasticity
L	Length of the plate
q	Electrostatic force between the plate and the electrode
w	Width of the plate
x	Distance along the plate

Symbols

Δ	Normalize tip deflection d/g
Φ	Mass flux per unit area

*Graduate Research Assistant.

†Assistant Professor, AIAA Member, mohseni@colorado.edu

I. Introduction

With recent progresss in microfabrication techniques, microfluidic devices have become commercially appealing due to their numerous applications in biotechnology and process engineering. Miniaturization often results in cost reduction by reducing the amount of samples and reagents used, automation, and increasing throughput. Lab-On-a-Chip[1] devices, Micro Total Analysis Systems[2] (μTAS), and microreactors[3] are among potential applications of microfluidic devices. In these applications the generic term mixing comprises a multitude of operations that target different tasks such as mixing, emulsification, blending, and suspension. Consequently an essential area in microfluidic research concerns mixing and dispersion of reagents, which can be small molecules, large macromolecules, particles, and bubbles and drops. Therefore, microscale mixing is crucial to effective performance of many microfluidic devices.[4] A common feature of the above-mentioned applications is to merge two or more streams of fluids being separated before. As a result, significant demands exist for faster, smaller, and more effective micromixers.

Mixing rate is characterized by the diffusion flux given by the Fick's law $\Phi = -D\ \nabla C$, where Φ is the mass flux per unit area, D is the diffusion coefficient, and ∇C is the concentration gradient. The net mass flow rate is proportional to the contact surface area. The more the contact surface, the higher the mixing rate. This is the essence of most micro-scale mixing techniques.

Conventionally, mixing of fluids at large scales involves generating turbulence. However, micromixers are commonly identified by small characteristic length and small velocity; resulting in low operational Reynolds numbers. In such cases, where turbulence is often absent, mixing is mainly achieved by molecular diffusion. Since diffusion is often a slow process, particularly in liquid media, various mechanisms for mixing in laminar flow regime have been suggested (see e.g., Ehrfeld *et al.*[3]). A key concept for enhancing microscale mixing is to increase the interface area between the two fluids. In this study, vortex formation and roll-up are suggested as an efficient technique to increase the contact area, and hence, increase mixing between two fluids (see Fig. 1).

Micromixers can be classified in two categories, passive and active. While external perturbations are introduced in active micromixers to enhance mixing, no external perturbation exists in passive micromixers. Passive micromixers can be categorized based on the arrangment of mixed phases to parallel or serial lamination,[5,6] injection,[7] chaotic advection,[8,9] and droplet micromixers.[10] The mixing process in passive mixers relies entirely on diffusion or chaotic advection. Decreasing the diffusion path between the mixing fluids and/or increasing the contact surface between them will enhace mixing. Lamination is a basic technique used in designing many passive micromixers, *e.g.* in,[11] where successive layers of fluids are separated and then recombined, resulting in several relatively thin layers of fluid. Chaotic advection is also explored in passive mixers to reduce the diffusion path, and consequently enhancing mixing. An interdigital glass micromixer was recently developed,[12,13,14] where improvement in mixing is achieved at the expense of excessive pressure drop along the channel and increased pumping power requirement. Liu *et al.*[8] created a 3-D serpentine microchannel design with a repeating "C-shaped" unit. The 3D nature of the flow in the channel introduces chaotic motion, resulting in improved mixing. Passive lamination and chaotic mixing are effective strategies to enhance mixing, however, by increasing the channel length they often result in significant increase in the pumping power requirement.

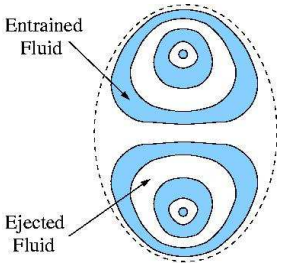

Figure 1. Fluid entrainment for effective mixing in a vortex pair formation.

Active micromixers can be categorized based on the nature of the external disturbances such as temperature,[15] pressure,[16] electrokinetics,[17,18] electrohydrodynamics,[19] dielectrophoretics,[20] magnetohydrodynamics,[21] and acoustics.[22] The structure and fabrication of active micromixers are often more complicated than passive micromixers and they require external power sources. However faster mixing rate with a shorter channel length has made active mixers the choice in many applications.[23]

There have been many design strategies for active micromixers. Deshmukh *et al.*[16,24] used two positive displacement pumps to design an integrated micromixer in order to drive the two fluids independently, where steam bubbles are utilized in the pump to generate fluid motion. The two fluids are alternately induced into the mixing channel when the pumps are operated out of phase. This results in a rapid mixing of the two fluids via dispersion. Ultrasonic vibration of a bulk piezoelectric lead-zirconate-titanate (PZT) ceramic is employed in the design of an ultrasonic micromixer by Yang *et al.*[25] A micromixer based on electroosmosis phenomena was suggested by Chen *et al.*[26] Ma *et al.*[27,28] developed electrostatically actuated MEMS planar flaps for enhancement of fluid mixing in gas environment. Bottausci *et al.*[29] considered an active chaotic advection micromixer where cross-stream secondary channels are used for time-dependent actuation. A time dependent electric field was used by Chen *et al.*[26] to take advantage of electroosmosis perturbation to mix fluids. There are excellent reviews of various aspects of mixing and micromixers. The reader is referred to, for example, Nguyen and Wu,[30] Ottino and Wiggins,[31] Stone *et al.*,[32] and Kakuta *et al.*[33] for further references.

This manuscript is organized as follows: In the next section the design concept of a resonant plate micropump-mixer is presented. Electromechanical design of the micropump-mixer is summarized in section III. Fabrication technique and assembly are outlined in section IV, while flow visualization technique and set-up are discussed in section V. Section VI contains data analysis and characterization of the mixing process. Finally, concluding remarks and future directions presented in section VII.

II. Micropump-mixer Design

Most available micromixers require long channel length, complicated design, and high pumping power. In this study, we present a new strategy for effective mixing. The key concept is that an increase in the area of the interface between two fluids would results to increased mixing. A resonant plate, preferably located at the interface between the two fluids, can constantly increase the interface area by perturbing the interface. The resonant plate create a compact shear and vortical region around the tip of the plate. As depicted in Fig. 1, vortex formation involves significant entrainment that can enhance mixing (see Fig. 1).

A resonant microfan for operation in gas environment was recently fabricated at the University of Colorado.[34,35] Resonant frequencies of 10-30 KHz was reported in air for a microfan operating 30 μm above a substrate. Linderman *et al.*[34,35] showed that the net induced gas flow by the microfan is dominated by the formation of vortices and a recirculation zone. A similar design is used in this study to fabricate a resonant plate for effective mixing and pumping of fluids, in particular in liquids.

An electrostatically activated resonant plate is used for pumping and mixing in both liquid and gas environments. The resonant plate is placed at or reasonably close to the interface between the two incoming fluid streams at the junction of a Y-shaped microchannel (see Fig. 2). An electrode lies on one side of the channel in the vicinity of the junction for actuation of the plate at its first resonant mode. Actuated resonant plate will disturb the shear layer at the interface of the two fluids, where it enhance vorticity generation. Consequently, an intense vortical region is generated around the tip of the resonant plate, and the resulted interface stretching would enhance mixing. In the mean time, the resonant plate will also pump the flow through the channel. This effect is similar to thrust generation by flapping wings of insects.[36,37] In summary, the resonant micropump-mixer of this study is effective in microscale mixing, while it could also pump the mixed fluids through the channel. This is an important feature that we would like to demonstrate in this investigation.

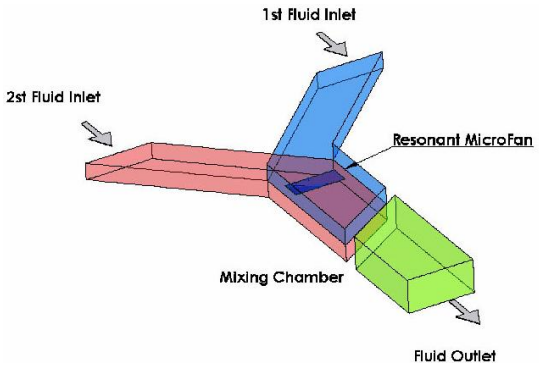

Figure 2. Resonant fan micropump-mixer design concept.

III. Electromechanical Design

Actuation at the natural frequency of the cantilevered plate is an important parameter in order to take advantage of the resonance of the plate for maximum actuation amplitude. Furthermore, the current electrostatic actuation design is susceptible to snap through. In this section models for predicting these quantities are presented. Such models will be used as a guide in the design of the resonant micropump-mixer.

Electrostatic Drive Voltage. At the snap-through voltage the nonlinear electrostatic forces overpower the linear mechanical resistance of the actuated plate and the device quickly flattens against the driving voltage. Therefore, the micropump-mixer ought to operate at a voltage below the snap-through value. In order to determine the snap-through voltage, the resonant plate is molded as a cantilever beam fixed at one end (see Fig. 3). Fluid damping effects are neglected in the current model. The electrostatic force $q(x)$ between the plate and the electrode depends on the deflection of the plate at any distance x, along the plate. Assuming a square-law curvature for the beam deflection, the load distribution along a plate of length L is given by[38]

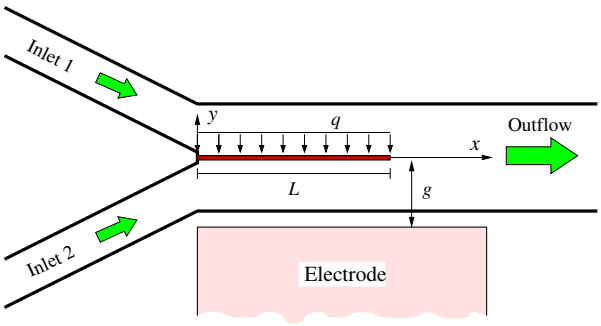

Figure 3. Microfan model for electromechanical analysis.

$$q = \frac{\epsilon_0 \epsilon_r w}{2} \left(\frac{V}{g - \bar{x}^2 d} \right)^2, \tag{1}$$

where $\bar{x} = x/L$, is the nondimensional distance along the plate, w is the width of the plate, g is gap between the plate and the electrode, and q is in N/m.

Using the conventional beam theory,[39] the tip deflection under partial loading is given by

$$d = \frac{1}{6EI} \int_0^L x^2 (3L - x) q(x) dx, \tag{2}$$

where $I = wh^3/12$ is the moment of inertia, E is the module of elasticity, and h is the thickness of the resonant plate. Combining equations (1) and (2) one can obtain

$$d = \frac{\epsilon_0 \epsilon_r w V^2}{12EI} \int_0^L (3L\,x^2 - x^3) \left(\frac{1}{g - \bar{x}^2 d} \right)^2, \tag{3}$$

The integral in equation (3) can be solved for the voltage[40] to obtain

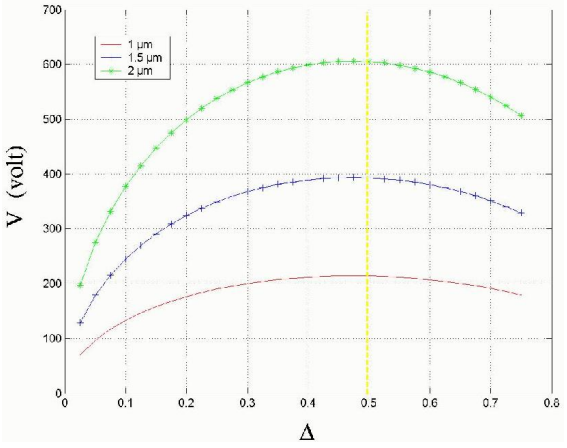

Figure 4. Driving voltage versus the normalized deflection for various plate thicknesses.

$$V = \sqrt{\frac{8\Delta^2 EIg^3}{\epsilon_0 \epsilon_r w L^4} \left(\frac{2}{3(1-\Delta)} + \frac{\tanh^{-1}\sqrt{\Delta}}{\sqrt{\Delta}} - \frac{\ln(1-\Delta)}{3\Delta} \right)^{-1}}, \tag{4}$$

where $\Delta = d/g$ is the normalize tip deflection. Therefore, the driving voltage for any given tip displacement can be calculated from the equation (4). Driving voltages for a silicon plate of length $L = 300$ μm at various

plate thicknesses between 1-2 μm are shown in Fig. 4. Note that normalized loads greater than 0.5 can not be realized as it exceeds the snap-through voltage.

First Resonant Frequency. The angular natural frequency of the resonant plate can be defined as[41]

$$f = \frac{W_n}{2\pi} = \frac{3.52}{2\pi}\sqrt{\frac{EI}{\bar{m}L^4}}, \tag{5}$$

where $\bar{m}$ is the distributed mass over the resonant plate. Figure 5 shows this relationship between the resonant frequency and the length of the plate for a few microfabricated test cases considered in this study. The resonant frequency drops sharply as the length of the plate is increased. The first resonant frequency of the plate is measured by the reflection of a laser beam from the free end of the resonant plate. The amplitude of the plate's deflection increases around the resonant frequency. This could cause the widening of the reflection pattern which results in measurement errors. Four different resonant plate prototypes with 300 μm length are fabricated and used to evaluate the accuracy of the model. The measured resonant frequency for these prototypes are found to be: Prototype 1: 11.1 kHz, Prototype 2: 12.2 kHz, Prototype 3: 10.9 kHz and Prototype 4: 10.7 kHz. Small variation in the frequency measurement can be explained by the increase in the amplitude of the plate's deflection around the resonant frequency, which results in widening of the reflection pattern.

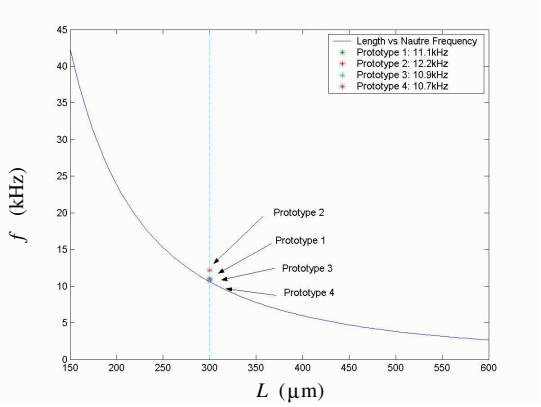

Figure 5. Resonant frequency versus the length of the plate. $g = 50\mu$m, $w = 600\mu$m, $E = 169$ GPa for Polysilicon, $\epsilon_0 = 8.85 \times 10^{-12}$ C^2/N m^2, and $\epsilon_1 = 1$ C^2/N m^2 for air.

IV. Micropump-mixer Fabrication and Assembly

Package and fabrication technique brings MEMS integration to a new level of design flexibility, however packaging is one of the major challenges of MEMS devices. MEMS packaging is more challenging than IC packaging due to the diversity of MEMS devices and the requirement that many of these devices be in contact with their environment. In order to consider the hermeticity issue in fluid environment, packaging become even more challenge in microfluidic device. In this research a particular fabrication processes are required in order to retain flow visualization capabilities inside the micropump-mixer. As shown in Fig. 6, the resonant micropump-mixer is fabricated and packaged from three individual components: 1st microchannel substrate, 2nd microchannel substrate, and a resonant plate.

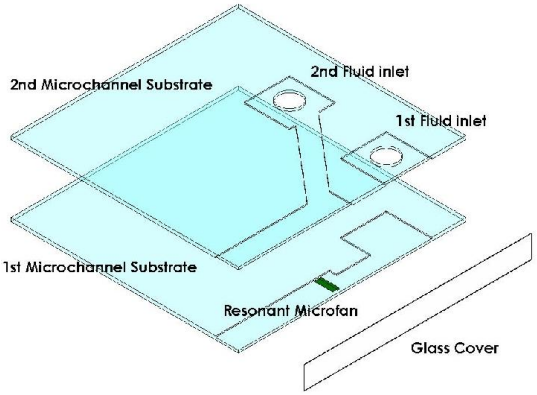

Figure 6. Resonant fan micropump-mixer design.

A. Resonant Microfan Design & Fabrication The fabrication process of the microfan is based on a similar design suggested by Linderman.[34,35] The two dimensional structure of the microfan can be easily fabricated using micro photolithography technology. A substrate with structure layer was supported by sacrificial layer. The sacrificial layer can be washed away using postprocessing steps and free the suspended structural layer on the substrate. The material used for the structure layer defining the fan plate must be conductive, or a combination of conductive and insulating materials in order to allow charge to flow into

the fan for electrostatic actuation. By using the commercial MUMPs process, the fan is designed based on PolyMUMPs, a three-layer polysilicon surface micromachining process. The resonant microfan design in the PolyMUMPs process is by using a single polysilicon layer (Poly 1 layer) for the fan plate and the second polysilicon layer (Poly 2 layer) as reinforcing rib to add further strengthen to the fan plate. A 0.5μm thick gold layer (Metal layer) is patterned as anchor bonding pad. The sacrifice layer (Oxide 1) is used to release the gold bumped substrate to the target substrate. A typical design for the resonant microfan using commercial PolyMUMPs is shown in Fig. 7(a). 5μm etch holes must be distributed across the fan plate at approximately 80μm intervals to allow the hydroflouric acid (HF) used during the release process for rapidly under etch. The layout of the microfan design is shown in Fig. 7(b).

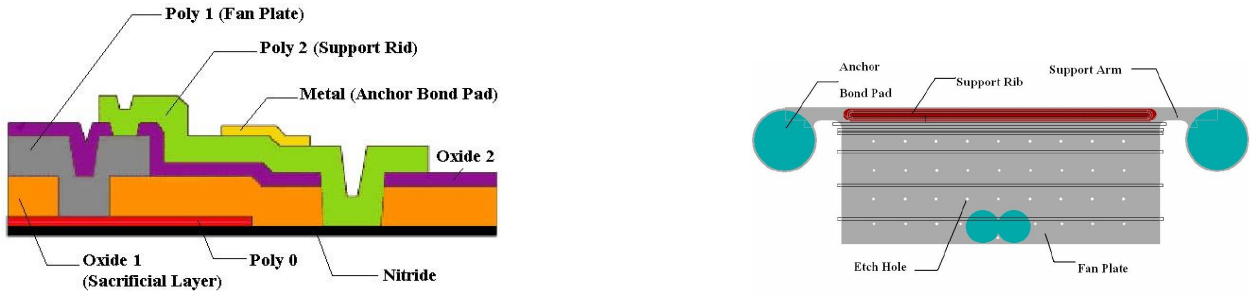

(a) (b)

Figure 7. Following[34,35] (a) Layout description for commercial PolyMUMPs process, (b) Resonant microfan layout.

B. Microchannel Design and Fabrication. In order to have a two incoming streams where the microfan sit in the middle and a clear side view to observe the mixing performance, two-layer microchannel structure is needed. The Y-Shaped microchannel presented here is made from SU-8. SU-8 is a widely used negative epoxy type near-UV photoresist that can be easily applied. SU-8 layers as thick as 2 mm with aspect ratios greater than 20 has been reported with standard contact lithography equipment.[42,43] SU-8 layers are applied and then patterned on a ceramic substrate for the 1st microchannel, and on glass substrate for the 2nd microchannel. In this study, SU-8 2100 is used in the fabrication of microchannels with a thickness of 200 μm. The microchannel design and layouts are shown in Fig. 8.

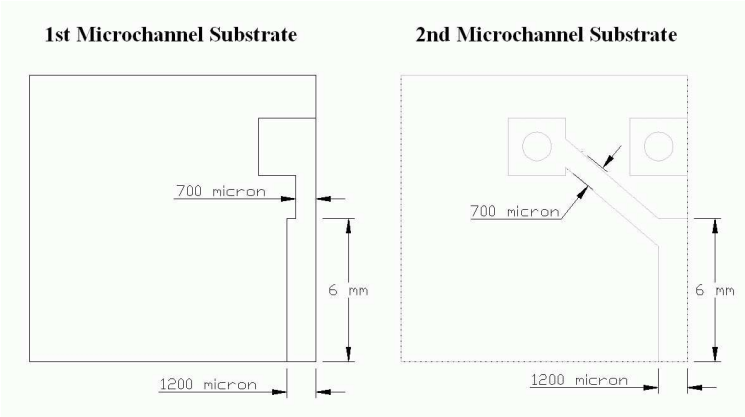

Figure 8. The 1st and the 2nd microchannel substrate layouts.

C. Resonant Micropump-Mixer Assembly. The gold-bumped resonant microfan chip is flip-chip bonded to the 1st microchannel substrate under 15 lb bonding force at 60°C. With the fan chip aligned and bonded to the target substrate, the system is placed in a Hydroflouric Acid (HF) bath to remove the sacrifical oxide layer, leaving the fans attached only to the substrate by gold bump anchors (see Fig. 6). The surface profile was measured using the ZYGO 3D Surface Profiler. The measurement shows that the height of the channel is around 300 μm and the anchor of the gold bump is around 35 μm.

The gap between the plate and the electrode is controlled by changing the bonding force. The resonant plate is, then, flip-chip bonded to the 1st microchannel substrate under 15 lb bonding force at 60 C. With the fan chip aligned and bonded to the target substrate, the system is placed in a Hydroflouric Acid (HF) bath to remove the sacrificial oxide layer, leaving the resonate plate attached only to the substrate by the gold bump anchors in the 1st microchannel substrate.

Using ZYGO 3D Surface Profiler, the height of the channel is found to be around 200 μm and the anchor of the gold bumps to be around 35 μm (See Fig. 10). After the resonant plate is bonded to the 1st microchannel substrate, the 1st substrate with the resonant plate is flip-chip bonded to the 2nd microchannel substrate. Both the 1st and the 2nd inlet channels are 700 μm $\times$ 200 μm , while the outlet channel is 1200 μm $\times$ 400 μm height. A UV adhesive (Norland Optical Adhesive 61) is used to seal a glass cover on the side for flow visualization. The complete fabricated resonant micropump-mixer is shown in Fig. 9, where the final size of the visualization prototype is 1.27 cm $\times$ 1.27 cm $\times$ 0.45 cm. Fig. 11 outlines the fabrication process flow chart of resonant micropump-mixer.

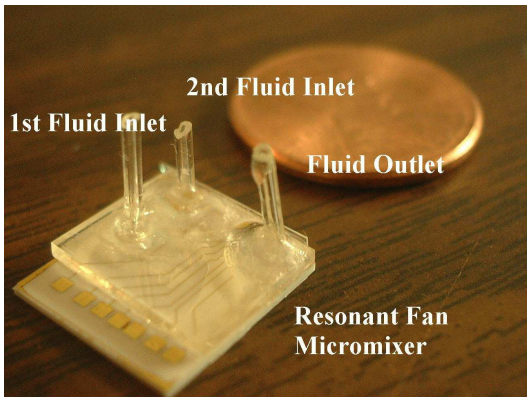

Figure 9. The resonant plate micropump-mixer.

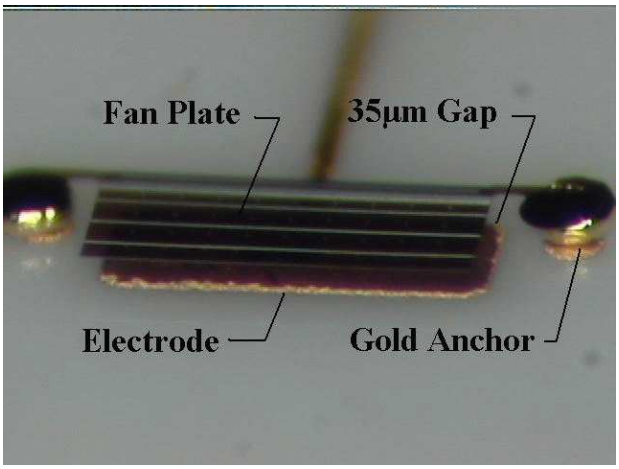

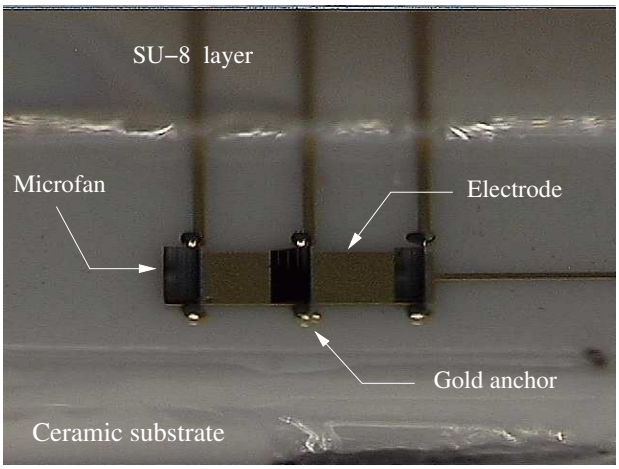

Figure 10. Flip-chip assembled resonant plate array on the 1st microchannel substrate with gold wiring and electrode.

V. Flow Visualization of Micromixing

In this study laser-induced fluorescence (LIF) technique[44] is used for flow visualization of the mixing process inside the resonant micropump-mixer. LIF is optical emission from molecules that have been excited to higher energy levels by absorption of electromagnetic radiation. The main advantage of fluorescence detection compared to absorption measurements is the greater sensitivity achievable because the fluorescence signal has a very low background. LIF provides selective excitation of the analyte to avoid interferences for molecules that can be excited resonantly. Since fluorescence emission intensity of the dye molecules is a passive scalar that can be measured for concentration variations inside the channel, LIF is an effective technique in characterizing mixing at microscale. A schematic of our experimental setup is shown in Fig.

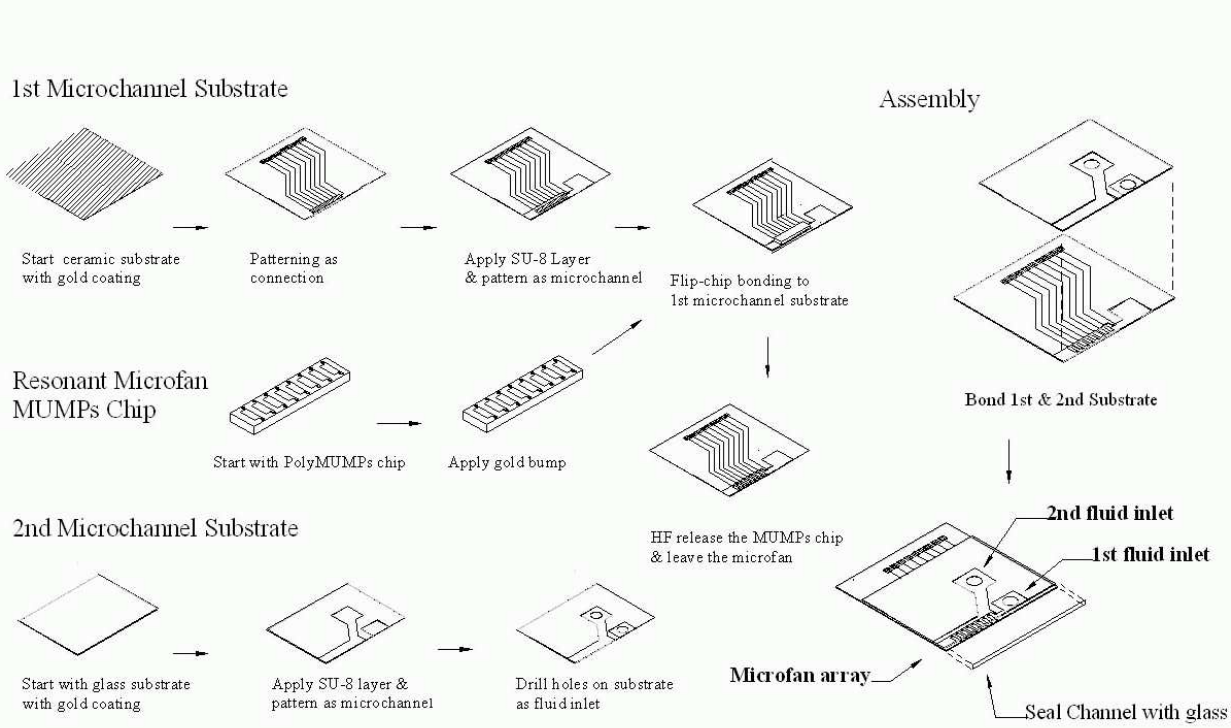

Figure 11. Fabrication process flow chart for the resonant micropump-mixer.

12. A Leica MS5 stereomicroscope attached to a PC and a CCD camera is used for imaging.

The excitation source for molecular LIF is typically a tunable dye laser in the visible spectral region. Our choice of the fluorescent dyes depends on the fluorescence excitation wavelengths of the laser (Nd:YAG laser: 532nm), the selected filter (Optical filter: 578∼633 nm), and the solubility in the water. To this end, aqueous solution of the fluorescent dye- Rhodamine WT (RWT), are used in this investigation. RWT diluted with deionized water (DI water) is pumped through the 1st fluid inlet while plain DI water is pumped through the 2nd fluid inlet. An automatic syringe pump is used to keep a laminar flow rate of 0.24ml/min through each channel. Mixing performance of the micropump-mixer is visualized by investigating the evolution of the fluorescence intensity across the channel width. Rhodamine WT fluorescent dye is excited by a light of a shorter wavelength (green). The emitted light is, then, at a longer wavelength; red in this case. The laser illumination is directed into the flow field through the microscope via a dichroic mirror. The optical filters are chosen so that only emitted light from the particles is transmitted to the CCD cameras. The cameras are coupled to the tereomicroscope via Optem 7:1 variable zoom tubes. The micropump-mixer is fixed on a 3-axis stage inside the field of view of the microscope.

VI. Mixing Analysis and Results

Mixing performance of a prototype resonant micropump-mixer is studied in this section. The prototype has a resonant plate of 300 μm length which is operated at its first resonant mode at 12 kHz with a 20 VAC power source. The resonant plate operates in a microchannel with the cross sectional dimension of 420 μm $\times$ 1200 μm. In this particular design, the distance between the first resonant plate and the initial contact line of the two streams is about 2mm.

Three consecutive snap shots of the flow in the outlet channel, with time intervals of 0.53 seconds, are shown in Fig. 13. Fig. 13(a) shows an organized laminar flow field before the actuation of the resonant plate starts. Due to the relative large distance between the initial contact line of the two flow streams at

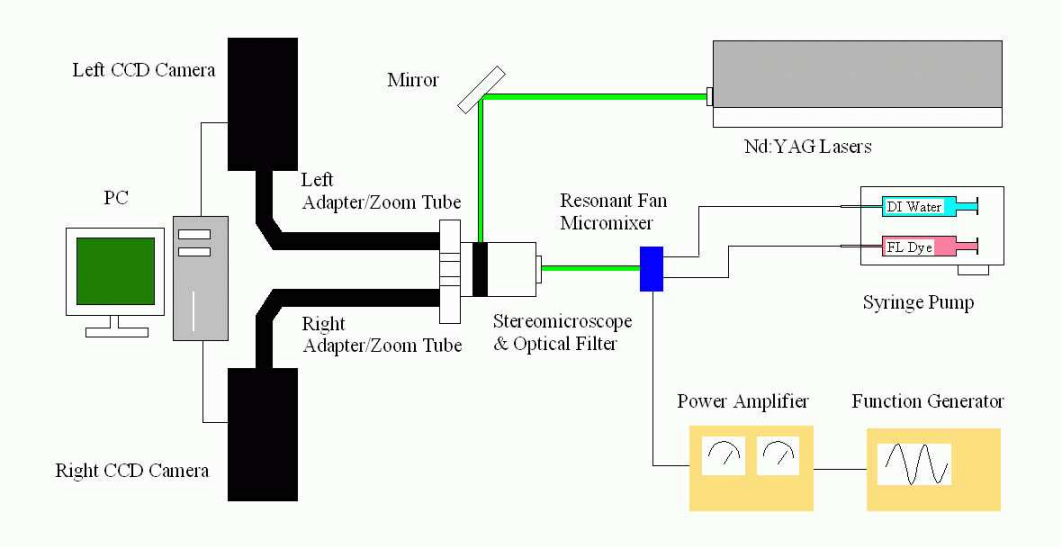

Figure 12. Schematic illustration of the experimental setup for Laser-induced fluorescence (LIF).

the Y-junction and the location of the resonant plate, some smearing of the interface concentration gradient is observed by molecular diffusion. Figures 13(b) and (c) show the flow field after the resonant plate is actuated. An almost instantaneous mixing is observed by operating the resonant plate. While, a microarray of resonant plates are fabricated, only one plate is actuated during the visualization. Actuation of multiple plates in the array results in more effective mixing and pumping.

Mixing enhancement is characterized by the measuring the intensity of the emitted light from the fluorescent dye. The images were viewed and processed using a Matlab image processing toolbox. The concentration at each point is then correlated to the local image intensity. The instantaneous normalized pixel intensities along the channel height are shown in Fig. 14(a, c, e). Since the distribution of the leaser beam intensity is non-uniform along the channel, a normalized intensity profiling is needed. The normalized intensity enables us to draw a correlation to the concentration profile, as the intensity is proportional to the amount of fluorescent dye inside any sample pixel region. In order to compare the mixing performance along the microchannel, three normalized intensity profiles were plotted along the microchannel. Three consecutive mixing steps (1-3) are shown in Fig. 13. The three intensity profiles were the entrance section in the upstream of the microfan (A-A'), the microfan section (B-B') and the exit section in the downstream of the microfan (C-C').

The normalized intensity profiles are plotted using the Matlab image processing toolbox as shown in Fig. 14. The horizontal axis shows the distance from the bottom of the channel (0 μm) to the top of the channel (420 μm) and the vertical axis shows the normalized intensity form 0 to 1.0. For same inlet flow

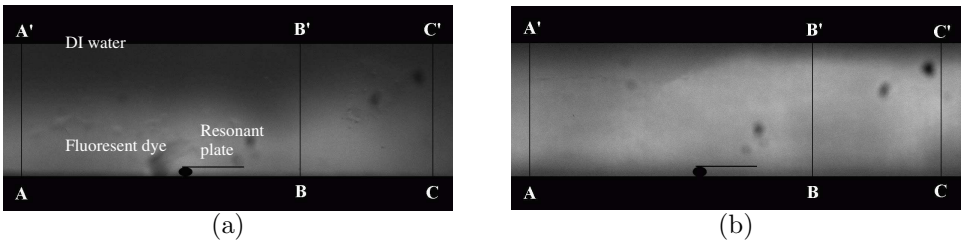

Figure 13. Imaging profile sections at times (a) 0 sec (b) 0.53 sec

rates, perfect mixing is achieved when the normalized intensity approaches 0.5 everywhere. When there is no external perturbation in the channel, mixing is a relatively slow process due to limited contact area of the two fluids; see Fig. 14(a). When the resonant plate is operating, it disturbs the flow field in the channel. Figure 14(c) shows the perturbation in the channel. Figure 14(e) shows that downstream of the resonant plate the normalized intensity is close to 0.5 across the channel, thus effective mixing is achieved. Intensity profiles plotted for the same cross section but at different times are shown in Fig. 14(b,d,f). These figures show that mixing is enhanced by the operation of the resonant plate. This is evident in both downstream and upstream from the fan.

VII. Conclusion

An electrostatically activated resonant plate is used in the design of an effective micropump-mixer in both liquid and gas media. A resonant micropump-mixer is fabricated and tested successfully by integrating the resonant plate in a Y-shaped microchannel. The interface between the two fluids is the most unstable location inside the channel; consequently an ideal place for actuation. The resonant plate must be located at or near the interface between the two fluids for optimal mixing. Mixing enhancement is observed due to perturbation of the shear layer between the two fluids at the tip of the resonant plate. A region of high vorticity concentration is generated around the tip of the plate where effective mixing in observed. Laser induced fluorescent technique is used for flow visualization and mixing characterization of deionized water and Rhodamine WT as the fluorescent dye. The resonant plate is activated at its first resonant frequency, in this case at 12 kHz. Effective mixing and pumping is observed.

Acknowledgments

The authors would like to thank Dr. Ryan J. Linderman and Dr. Oyvind H. Nilsen for providing the details of their resonant microfan design in.[34,35] Dr. Jean Hertzberg generously provided some of the visualization equipment and set up for this study, and John Paul Giardino helped the flow visualization experiment.

References

[1]Oosterbroek, R. E., van Den Berg, A., and van Den Berg, A., *Lab-on-a-Chip : Miniaturized Systems for (Bio)Chemical Analysis and Synthesis*, Elsevier Science, 2003.

[2]Manz, A., Graber, N., and Widmer, H., "Miniaturized total chemical analysis systems: A novel concept for chemical sensing," *Sensors and Actuators, B*, Vol. 1, 1990, pp. 244–248.

[3]Ehrfeld, W., Hessel, V., and Lowe, H., *Microreactors: New Technology for Modern Chemistry*, Wiley-VCH, Weinheim, 2000.

[4]Knight, J., "Honey, I shrank the lab." *Nature*, Vol. 418, 2002, pp. 474–475.

[5]Branebjerg, J., Gravesen, P., and Krog, J., "Fast mixing by lamination," *MEMS' 96*, San Diego, CA, 11-15 February 1996, pp. 441–446.

[6]Koch, M., Witt, H., Evans, A., and Brunnschweiler, A., "Improved characterization technique for micromixers," *J. Micromech. and Microeng.*, Vol. 9, No. 2, 1999, pp. 156–158.

[7]Miyake, R., Lammerink, T., Elwenspoek, M., and Fluitman, J., "Micro mixer with fast diffusion," *MEMS' 93*, Fort Lauderdale, FL, 7-10 February 1993, pp. 248–253.

[8]Liu, R., Stremler, M., Sharp, K., Olsen, M., Santiago, J., Adrian, R., Aref, H., and Beebe, D., "Passive mixing in a three-dimensional serpentine microchannel," *J. MEMS*, Vol. 9, No. 2, 2000, pp. 190–197.

[9]Stroock, A., Dertinger, S., Ajdari, A., Mezic, I., G.M., H. S., and Whitesides, "Chaotic mixer for microchannels," *Science*, Vol. 295, 2002, pp. 647–651.

[10]Hosokawa, K., Fujii, T., and Endo, I., "Droplet-based nano/picoliter mixer using hydrophobic microcapillary vent," *IEEE MEMS '99*, 1999, pp. 388–392.

[11]Koch, M., Chatelain, D., Evans, A., and Brunnschweiler, A., "Two simple micromixers based on silicon," *J. Micromech. and Microeng.*, Vol. 8, No. 2, 1998, pp. 123–126.

[12]Hessel, V., Dietrich, T., Freitag, A., Hardt, S., Hofmann, C., Lowe, H., Pennemann, H., and Ziogas, A., "Fast mixing

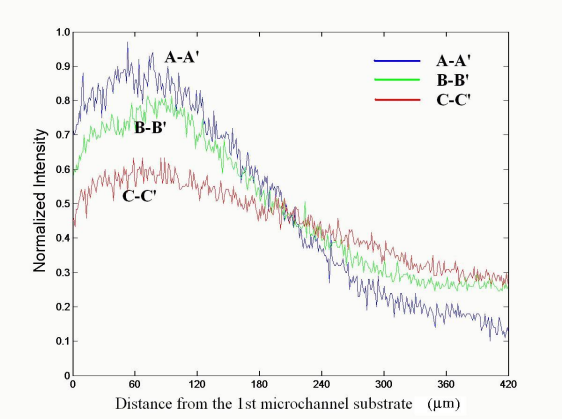

(a)

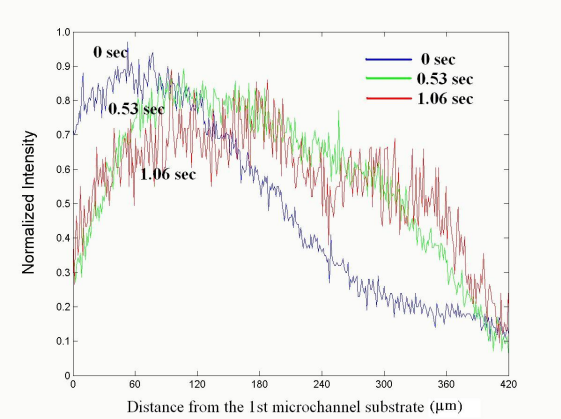

(b)

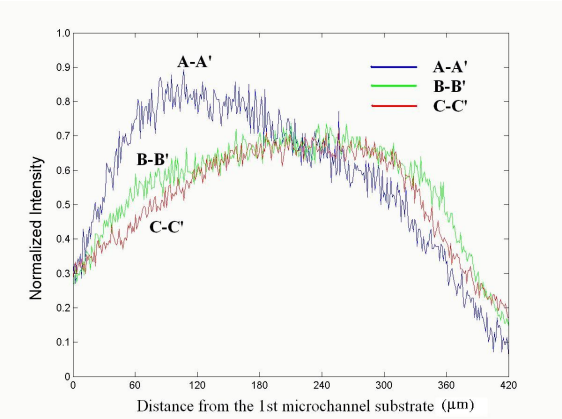

(c)

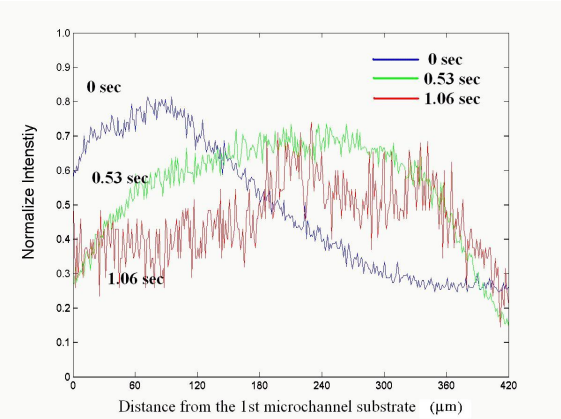

(d)

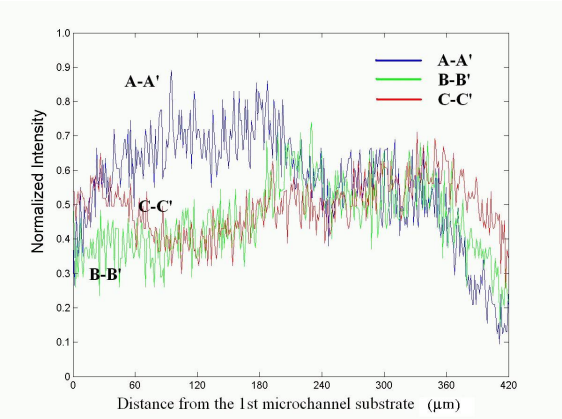

(e)

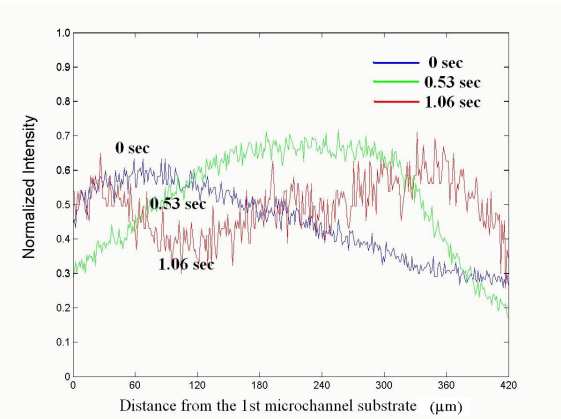

(f)

Figure 14. Intensity profiles at the same time but different cross sections of the channel. (a) $t = 0$, (c) $t = 0.53$, and (e) $t = 1.06$. Intensity profiles at the same cross section of the channel but at different times (b) Section A-A' (d) Section B-B' and (f) Section C-C'.

in interdigital micromixers achieved by means of extreme focusing," *Proceedings of IMRET6: 6th Int. Conf. Microreaction Technology*, New Orleans, March 10-14 2002.

[13]Hessel, V., Hardt, S., Lowe, H., and Schonfeld, F., "Laminar mixing in interdigital micromixers with different mixing chambers - Part I: Experimental characterization," *AIChE J.*, Vol. 49, No. 3, 2003, pp. 566–577.

[14]Hardt, S. and Schonfeld, F., "Laminar mixing in interdigital micromixers with different mixing chambers - Part II: Numerical simulations," *AIChE J.*, Vol. 49, No. 3, 2003, pp. 578–584.

[15]Tsai, J. and Lin, L., "Active microfluidic mixer and gas bubble filter driven by thermal bubble micropump," *Sensors and Actuators A*, Vol. 97-98, 2002, pp. 665–671.

[16]Deshmukh, A., Liepmann, D., and Pisano, A., "Continuous Micromixer with Pulsatile Micropumps," *Solid-State Sensor & Actuator Workshop*, Hilton Head, S.C., June 4-8, 2000.

[17]Jacobson, S., McKnight, T., and Ramsey, J., "Microfluidic devices for electrokinematically driven parallel and serial mixing," *Anal. Chem.*, Vol. 71, 1999, pp. 4455–4459.

[18]Oddy, M., Santiago, J., and Mikkelsen, J., "Electrokinetic instability micromixing," *Anal. Chem.*, Vol. 73, 2001, pp. 5822–5832.

[19]Moctar, A. E., Aubry, N., and Batton, J., "Electrodynamic micro-fluidic mixer," *Lab on a Chip*, Vol. 3, 2003, pp. 273–280.

[20]Deval, J., Tabeling, P., and Ho, C., "A Dielectrophoretic Chaotic Mixer," *MEMS' 02*, 2002, pp. 36–39.

[21]Bau, H., Zhong, J., and Yi, M., "A minute magneto hydrodynamic (MHD) mixer," *sensors Actuators B*, Vol. 79, 2001, pp. 207–215.

[22]Zhu, X. and Kim, C., "Acoustic-Wave Liquid Mixer," *Proceeding of the ASME Symposium on Mechanics in Micro-Electro-Mechanical Systems*, Vol. DSC-Vol. 62, Dallas, TX, November 16-21 1997, pp. 32–35.

[23]Nguyen, N.-T. and Wereley, S., *Fundamentals and Applications of Microfluidics*, Artech House, Inc., Norwood, MA, 2002.

[24]Deshmukh, A., Liepmann, D., and Pisano, A., "Characterization of a micro-mixing, pumping, and valving system," *Proceedings of the 11th Int. Solid-State sensors & Actuators*, Munich, Germany, 2001, pp. 950–953.

[25]Yang, Z., Matsumoto, S., Goto, H., Matsumoto, M., and Maeda, R., "Ultrasonic micromixer for microfluidic systems," *Sensors and Actuators A*, Vol. 93, 2001, pp. 266–272.

[26]Chen, H., Zhang, Y., Mezic, I., Meinhart, C., and Petzold, L., "Numerical simulation of an electroosmotic micromixer," *Proceedings of the Int. Mech. Eng. Congress & Exposition*, ASME, Washington, D.C., November 15-21 2003.

[27]Ma, Z., Chen, X., and Lee, Y., "Electrostatic Planar fan enhancement of fluid mixing," *Int. J. of Nonlinear Sciences and Numerical Simulations*, Vol. 3, No. 3-4, 2002, pp. 277–283.

[28]Ma, Z., Peacock, T., Bradley, E., and Lee, Y., "Solder-assembled MEMS flaps to enhance fluid mixing," *Proceedings of the ASME Int. Mech. Eng. Congress and Exposition*, New York, NY, November 11-16 2001.

[29]Bottausci, H., Cardonne, C., Mezic, I., and Meinhart, C., "An actively controlled micromixer: 3-D aspect," *Proceedings of the CISM Microfluidics History, Theory and Applications*, ASME, Udine, Italy, 2003.

[30]Nguyen, N.-T. and Wu, Z., "Micromixers – a review," *J. Micromech. Microeng.*, Vol. 15, 2004, pp. R1–R16.

[31]Wiggins, S., "Introduction: mixing in microfluidics," *Phil. trans. R. Soc. Lond. A*, Vol. 362, 2004, pp. 923–935.

[32]Stone, H., Stroock, A., and Ajdari, A., "Engineering flows in small devices," *Ann. Rev. Fluid Mech.*, Vol. 36, 2004, pp. 381–411.

[33]Kakuta, M., Bessoth, F., and Manz, A., "Microfabricated devices for fluid mixing and their application for chemical synthesis," *Chem. Rec.*, Vol. 1, 2001, pp. 395–405.

[34]Linderman, R., Sett, S., and Bright, V., "The Resonant Micro Fan For Fluidic Transport, Mixing And Particle Filtering," *Proceedings of the 2001 ASME International Mechanical Engineering Congress and Exposition*, 2001.

[35]Linderman, R., Nilsen, O., and Bright, V., "The Resonant Micro Fan For Fluidic Transport, Mixing And Particle Filtering," *Proceedings of the 12th Int. Conference on Solid-State Sensors, Actuators and Microsystems,*, Boston, MA, June 8-12 2003.

[36]Lighthill, M., "On the Weis-Fogh mechanism of lift generation," *J. Fluid Mech*, Vol. 60, No. part 1, 1973, pp. 1–17.

[37]Maxworthy, T., "Experiments on the Weis-Fogh mechanism of lift generation by insects in hovering flight," *J. Fluid Mech*, Vol. 93, No. part1, 1979, pp. 47–53.

[38]Senturia, S., *Microsystem Design*, Kluwer Academic Publishers, 2000.

[39]Gere, J. and Timoshenko, S., *Mechanics of Materials*, PWS Pub. Co., 4th ed., 1997.

[40]Peterson, K., "Dynamic Micromechanics on Silicon: Techniques and Devices," *IEEE Trans. Electron Devices*, Vol. 25, 1978, pp. 1241–1250.

[41]Harris, C. and Piersol, A., *Shock and Vibration Handbook*, McGraw-Hill Book Co., 5th ed., 2001.

[42]Corp., M., http://www.microchem.com/products/ su_eight.htm.

[43]Tay, F., van Kan, J., Watt, F., and Choong, W., "A novel micro-machining method for the fabrication of thick-film SU-8 embedded micro-channels," *Journal of Micromechanics and Microengineering*, Vol. 11, No. 1, 2001, pp. 20–26.

[44]Smits, A. and Lim, T., *Flow Visualization: Techniques and Examples*, World Scientific Publishing Company, 2000.